Carbohydrate Polymers 101 (2014) 444–450

Contents lists available at ScienceDirect

Carbohydrate Polymers

journal homepage: www.elsevier.com/locate/carbpol

Acylation of cellulose in a novel solvent system: Solution of dibenzyldimethylammonium fluoride in DMSO

Romeu Casarano, Paulo A.R. Pires, Omar A. El Seoud*

Institute of Chemistry, University of São Paulo, P.O.B. 26077, 05513-970 São Paulo, Brazil

ARTICLE INFO

Article history:
Received 3 July 2013
Received in revised form 2 September 2013
Accepted 14 September 2013
Available online 21 September 2013

Keywords:
Cellulose acylation
Dibenzyldimethylammonium fluoride-hydrate
Molecular dynamics
Tetra(1-butyl)ammonium fluoride-hydrate

ABSTRACT

A novel electrolyte, dibenzyldimethylammonium fluoride has been obtained essentially anhydrous (BMAF-0.1H_2O) by a simple route. Its thermal stability, relative to tetra(1-butyl)ammonium fluoride trihydrate (TBAF—3H_2O) has been demonstrated by thermogravimetric analysis. DMSO solution of (BMAF-0.1H_2O) dissolves microcrystalline- and fibrous celluloses; the dissolved biopolymers have been acylated by ethanoic-, butanoic-, and hexanoic anhydride. The degrees of substitution of the esters are higher than with TBAF—3H_2O/DMSO. The reasons are discussed in terms of differences in electrolyte structure and contents of water of hydration, whose presence leads to side reactions and decreases of the basicity of (F^-). This conclusion is corroborated by molecular dynamics simulations of the interactions of glucose dodecamer/R_4NF-hydrate/DMSO. These show that the interactions oligomer-F^--water is operative only for TBAF—3H_2O/DMSO. The efficiency of BMAF-0.1H_2O/DMSO is explained based on better accessibility of the biopolymer due to efficient hydrogen-bonding between its hydroxyl groups and the essentially desolvated (F^-).

1. Introduction

Quaternary ammonium fluoride hydrates (R_4NF-hydrates) in aprotic solvents (e.g., DMSO and THF) have been used as deprotecting agents and source of (F^-) in organic synthesis, e.g., in desilylation, cyclization, conjugate addition, acylation, alkylation, condensation, and elimination (Fieser, 1967; Pliego & Pilo-Veloso, 2008; Sun & DiMagno, 2005, 2006). Tetra(1-butyl)ammonium fluoride trihydrate (TBAF—3H_2O)/DMSO has been employed for cellulose dissolution and its subsequent derivatization, into, e.g., carboxylic acid esters (Casarano, Nawaz, Possidonio, da Silva, & El Seoud, 2011; Heinze & Koehler, 2010; Leibert & Heinze, 2005), ethers (Heinze, Wanga, Koschella, Sullob, & Foster, 2012; Heinze, Lincke, Fenn, & Koschella, 2008), and for regioselective deacylation of carboxylic esters (Xu & Edgar, 2012; Zheng, Gandour, & Edgar, 2013). The small volume and high charge density of (F^-) play an important role in the efficiency of this solvent system because hydrogen-bonding between the anion and the hydroxyl groups of the anhydroglucose units, AGU, of the biopolymer disrupts the strong intermolecular bonding present, leading to its dissolution.

The use of (R_4NF-hydrates/DMSO) is not, however, without limitations, see parts (A–E) of Scheme 1. Depending on the strength of association between the constituent ions, the electrolyte may not dissolve cellulose, e.g., tetramethylammonium fluoride, or its efficiency is low, benzyltrimethylammonium fluoride-H_2O (Koehler & Heinze, 2007). The associated water of hydration leads to hydrolysis of the acylating agent (Ass, Frollini, & Heinze, 2004; Xu, Li, Tate, & Edgar, 2011), combined with a decrease of the degree of substitution, DS, of the produced ester. This occurs via a general base catalyzed hydrolysis (Scheme 1A), and/or a ketene intermediate (Scheme 1B) (Casarano et al., 2011; Zheng et al., 2013). The electrolyte itself may undergo elimination reactions, including Hofmann elimination (Scheme 1C) (Albanese, Landini, & Penso, 1998; Sharma & Fry, 1983) and/or degradation via an ylide intermediate, akin to the E1cB mechanism, except that the species generated is a zwitterion, and not an anion (Scheme 1D) (Chempath, Boncella, Pratt, Henson, & Pivovar, 2010; Makosza & Chesnokov, 2003). Finally, tetraallylammonium fluoride-monohydrate (TAAF—H_2O), undergoes polymerization to form linear- as well as cross-linked cyclopolymers, that do not dissolve cellulose (Scheme 1E) (Casarano et al., 2011). Note that the synthesis of anhydrous TBAF by the reaction of C_6F_6 with tetra(1-butyl)ammonium cyanide is not a satisfactory solution to the water-mediated side reactions, because one of the reagents is expensive (US$ 25.6/g $(C_4H_9)_4$NCN, Sigma Aldrich); the resulting solution in DMSO (a mixture of $C_6(CN)_6$ and TBAF) is not stable; it does not dissolve cellulose after storage for 28 h at room temperature, RT (Koehler & Heinze, 2007).

In summary, although R_4NF-hydrates in DMSO are efficient solvents for cellulose, their use is hampered by the above-mentioned

---

* Corresponding author. Tel.: +55 11 3091 3874; fax: +55 11 3091 3874.
E-mail address: elseoud@usp.br (O.A. El Seoud).

0144-8617/$ – see front matter © 2013 Elsevier Ltd. All rights reserved.
http://dx.doi.org/10.1016/j.carbpol.2013.09.043

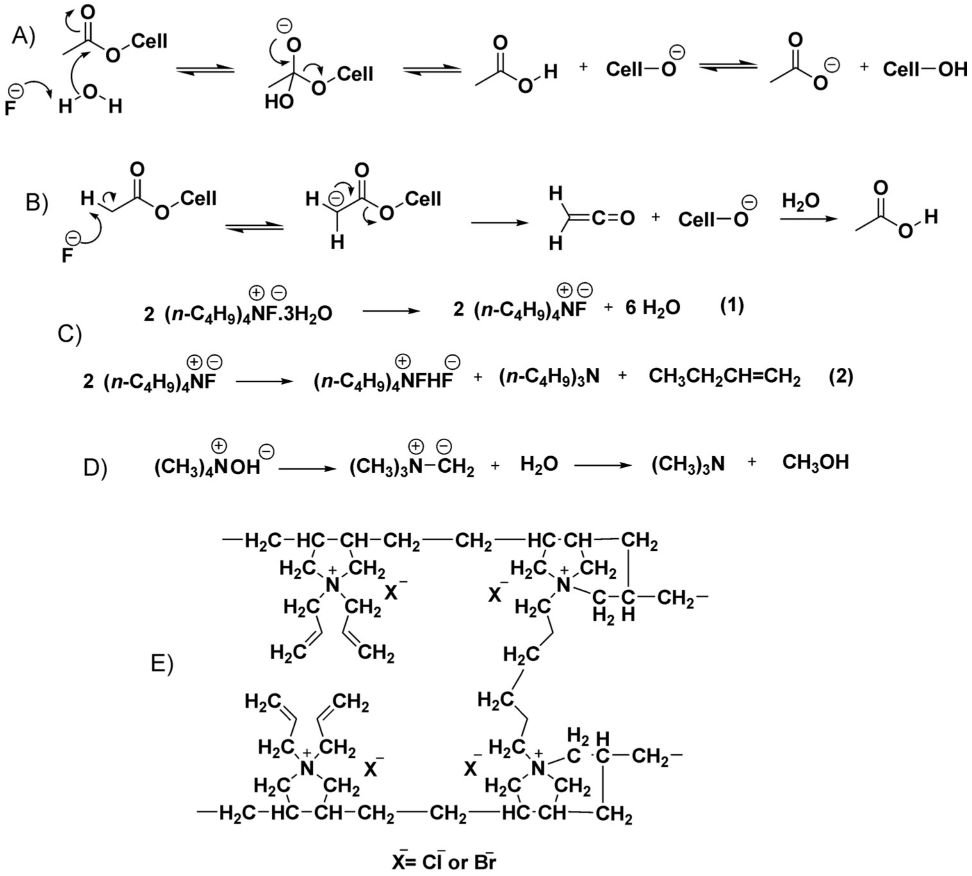

Scheme 1. Possible side reactions of tetraalkylammonium fluoride-hydrates. The schemes are for ester deacylation by the water of hydration, where the (F^-) is acting as a general-base (1A); ester deacylation via ketene intermediate (1B); electrolyte degradation by Hofmann elimination (1C); electrolyte degradation via ylide mechanism (1D); electrolyte polymerization/crosslinking (1E).

problems. Therefore, the search for a thermally stable quaternary ammonium fluoride with low water content is important, not only for cellulose chemistry, but also for organic synthesis.

We report here on an electrolyte, dibenzyldimethylammonium fluoride, that is easy to obtain in practically anhydrous form (BMAF-0.1H_2O) with satisfactory thermally stability (Casarano & El Seoud, 2013). A solution of this electrolyte in DMSO was found to be an efficient medium for dissolution and acylation of cellulose under homogeneous reaction conditions. The DS values obtained for cellulose esters were larger than those obtained in TBAF—3H_2O/DMSO and TAAF—H_2O/DMSO. The results of molecular dynamics (MD) simulations for the system glucose dodecamer (hereafter designated as "oligomer")/R_4NF-hydrate/DMSO showed that the oligomer-F^--water interactions are operative only for TBAF–3H_2O/DMSO. This explains the relative efficiency of BMAF-0.1H_2O/DMSO as solvent for cellulose, because the essentially desolvated (F^-) binds efficiently to the hydroxyl groups of the AGU leading, most certainly, to better accessibility, hence higher reactivity of the biopolymer chains.

2. Experimental

2.1. Materials

The reagents were purchased from Alfa Aeser or Merck and were purified, where required, as described elsewhere (Armagero & Chai, 2003). Microcrystalline cellulose, MCC; Avicel PH 101 was from FMC (Philadelphia; viscosimetric degree of polymerization, $DP_v = 175$). Cotton sheets (Nitro Química S.A., São Paulo) were cut into stripes, grounded, and sieved (100–200 mesh); $DP_v = 920$.

2.2. Equipment

The value of DP_v was determined by using a shear-dilution Cannon-Fenske viscosimeter (Schott), inserted in Schott AVS 360 automatic viscosity determination equipment. ^1H- and ^{13}C NMR measurements were recorded with Varian Innova-300 spectrometer (300 MHz for ^1H). Elemental analysis was performed with Perkin-Elmer Elemental Analyzer CHN 2400. Melting points were determined with either Electrothermal IA 6304 mp equipment (dibenzyldimethylammonium bromide hydrate, BMABr-hydrate) or TA Instruments DSC Q10 Differential Scanning Calorimeter (BMAF-hydrate). Thermogravimetric (TG) analyses were performed with TA Instruments Hi-Res TG 2950 Thermogravimetric Analyzer.

2.3. Material characterization

DP_v was determined (25 °C) from the intrinsic viscosity of cellulose solution in CUEN/water (1:1, v/v) according to the recommended procedure (ASTM, 2007). The DS of the cellulose carboxylic esters was determined by the back-titration method (ASTM, 2004).

2.4. NMR and thermal analyses

DMSO-d_6 was used as solvent for ^1H and ^{13}C NMR measurements.

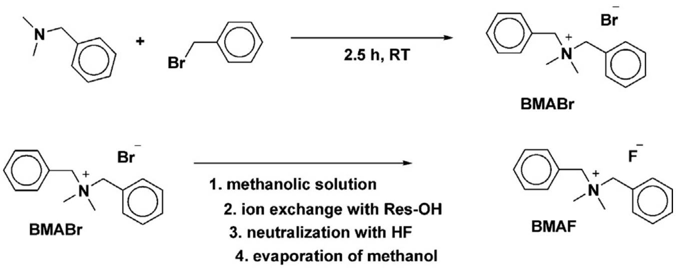

Scheme 2. Synthesis of BMAF-hydrate. First, BMABr-hydrate is synthesized, and then converted into the corresponding hydroxide, neutralized with HF, followed by methanol evaporation.

Thermal analyses have been carried out under the following conditions:

- Differential scanning calorimetry (DSC): N_2 atmosphere, 100 mL min^{-1}; sample mass = 6.0 mg; heating rate, 10° min^{-1}; T range = 25–160 °C; The DSC cell was calibrated with In (mp = 156.6 °C; $\Delta H_m = 28.59\,J\,g^{-1}$) and Zn (mp = 419.6 °C; $\Delta H_m = 111.40\,J\,g^{-1}$);
- TG: Isothermal TG, N_2 atmosphere, 50 mL min^{-1}; sample mass = 8.1 mg; T = 80 °C; 18 h; TG experiments, N_2 atmosphere, 50 mL min^{-1}; sample mass = 11.5 mg; T range from 35 to 600 °C; heating rate = 10 °C min^{-1}.

2.5. Synthesis of BMAF-hydrate

Scheme 2 illustrates the synthesis of BMAF-hydrate.

The synthesis of BMABr-hydrate was carried out as follows: benzyl bromide (25 mL; 0.21 mol) was added drop wise (ca. 15 min) to cold (ca. −10 °C) *N*,*N*,*N*-dimethylbenzylamine (30.0 mL; 0.20 mol) under constant, vigorous stirring and N_2 atmosphere, followed by reaction during 2.5 h, at RT. Toluene was added, the solid product filtered off, suspended several times in the same solvent and filtered off. The product was dried under reduced pressure, in the presence of P_4O_{10}. Yield 93%; white powder; mp = 172–173 °C; literature, mp = 176–177 °C (Erling & Gary, 1967; Karoly & Gyermek, 1952) and 175 °C (Busi, Lahtinen, Ropponen, Valkonen, & Rissanen, 2004). ^1H NMR (DMSO-d_6): δ (in ppm): 7.64–7.61 (*m*, 4H), 7.57–7.50 (*m*, 6H), 4.69 (*s*, 4H), 2.89 (s, 6H), where δ, *m*, and *s* stand for chemical shift, multiplet, and singlet, respectively; ^{13}C NMR (DMSO-d_6): δ (in ppm): 133.1, 130.3, 128.9, 128.0, 66.8, and 48.0. Both spectral data are in agreement with the literature (Busi et al., 2004). Elemental analysis (sample dried for additional 48 h, under reduced pressure, at 40 °C, in the presence of P_4O_{10}): Anal. Calcd. for $C_{16}H_{20}NBr$: C, 62.7; H, 6.6; N, 4.6%. Found: C, 62.5; H, 6.8; N, 4.6%.

BMAF-hydrate was obtained as follows: a methanolic solution of BMABr-hydrate (0.1 mol L^{-1}, 1 L) was passed through a column containing macroporous resin (Purolite SGA55OOH; 1.10 eq OH^-/L; 170 mL). The completeness of the (Br^-/OH^-) ion-exchange was assured by treating a sample of the eluent with $AgNO_3$ solution, acidified with nitric acid. The pH of the methanolic hydroxide solution was adjusted to ca. 7 (expanded-scale pH-paper) by adding methanolic/HF solution. Methanol was removed by evaporation; the pressure was gradually reduced from 200 to 10 mmHg at 50 °C, then to 2 mmHg, at 60 °C for ca. 4 h. The solid residue was additionally dried under reduced pressure (3 mmHg) for 48 h at 40 °C, in the presence of P_4O_{10}. White powder; mp = 132–133 °C. ^1H NMR (DMSO-d_6): δ (in ppm): 7.66–7.63 (*m*, 4H), 7.57–7.48 (*m*, 6H), 4.72 (*s*, 4H), 2.89 (*s*, 6H); ^{13}C NMR (DMSO-d_6): δ (in ppm): 134.0, 130.8, 129.5, 129.0, 67.7, and 48.6.

2.6. Determination of the water of hydration of BMABr and BMAF

The water contents of these electrolytes were calculated from the corresponding ^1H NMR spectra, by comparing the area of the water peak with that of known hydrogen of the electrolyte: H-8 of BMABr, Fig. SM-1a (Fig. 1a of Supplementary Material); H-8 of BMAF, Fig. SM-1b. These calculations indicated the following compositions: BMABr-0.5H_2O and BMAF-0.1H_2O.

2.7. Dissolution and acylation of cellulose in BMAF-0.1H_2O/DMSO

A clear, isotropic solution was obtained by stirring the electrolyte (3.3 g; 13.35 mmol BMAF) in DMSO (40 mL; 0.56 mol; always freshly distilled from CaH_2) for 15–30 min at 60 °C. MCC or cotton cellulose (0.50 g; 3.09 mmol) was introduced into the above-prepared solvent system, the suspension was heated at 80 °C for 20–40 min, under mechanical stirring, 570 ± 10 rpm. Cellulose dissolution was followed visually by placing a lamp behind the reaction flask; clear solutions were obtained in all cases. The required volume of acid anhydride was added, and the mixture was kept under the above-mentioned experimental conditions during the required length of time, vide infra. The resulting solution was poured into hot ethanol (60 °C, 400 mL); the suspension was stirred for 30–60 min; the precipitated solid was centrifuged at 3500 × g (IEC Centra 244 MP4R). This procedure was repeated three more times, the product was dried under reduced pressure at 50–60 °C, for 48 h, in the presence of P_4O_{10}, and its DS determined.

3. Results and discussion

3.1. Synthesis and water content of BMAF-hydrate

BMABr was synthesized by reacting neat *N*,*N*,*N*-dimethylbenzylamine and benzyl bromide for ca. 2.5 h at RT, with 93% yield. The reaction conditions/yield are superior to those reported elsewhere, e.g., the reaction of benzyl bromide, potassium carbonate, and DMF, 80 °C, 48 h, 52% yield, (Busi et al., 2004), or the reaction of benzyl bromide and *N*,*N*,*N*-dimethylbenzylamine, −10 °C, 3 days at RT, no yield reported (Tutaj, Gonzalez-Perez, Czapkiewicz, Del Castillo, & Rodriguez, 2001). ^1H NMR analysis indicated that the product is BMABr-0.5H_2O. Essentially anhydrous fluoride, BMAF-0.1H_2O, was obtained after ion-exchange ($Br^- \rightarrow OH^-$), neutralization of BMAOH with HF, methanol evaporation, and further drying.

3.2. Discussion of the side reactions occurring during the syntheses of R_4NF-hydrates

As mentioned above, TAAF–H_2O and TBAF–3H_2O are susceptible to polymerization/crosslinking and Hofmann elimination, respectively. The final stage in the synthesis of the former electrolyte involves neutralization of the methanolic TAAOH solution with HF, followed by evaporation of the alcohol. In order to avoid polymerization, (time consuming) solvent evaporation was carried out under reduced pressure at RT, or at higher temperature in the presence of a free radical scavenger, propyl gallate (Casarano et al., 2011). Almost anhydrous TBAF can be obtained by heating commercial TBAF–3H_2O at 40–45 °C, under reduced pressure for a long time 48–147 h; the products were found to contain from 0.1 to 0.3 H_2O/TBAF (Cox, Terpinski, & Lawrynowicz, 1984; Sharma & Fry, 1983). Freshly prepared almost anhydrous TBAF is not, however, stable at RT, even in solution, and should be used immediately. E.g., during its storage (as a solid) under reduced pressure, the concentration of bifluoride ion (HF_2^-, see Scheme 1 C), increased from 13 mol% to ca. 80 mol% after 4 days. On standing in CD_2Cl_2 solution, the concentration of (HF_2^-) reached 61- and 100 mol% after 3 and

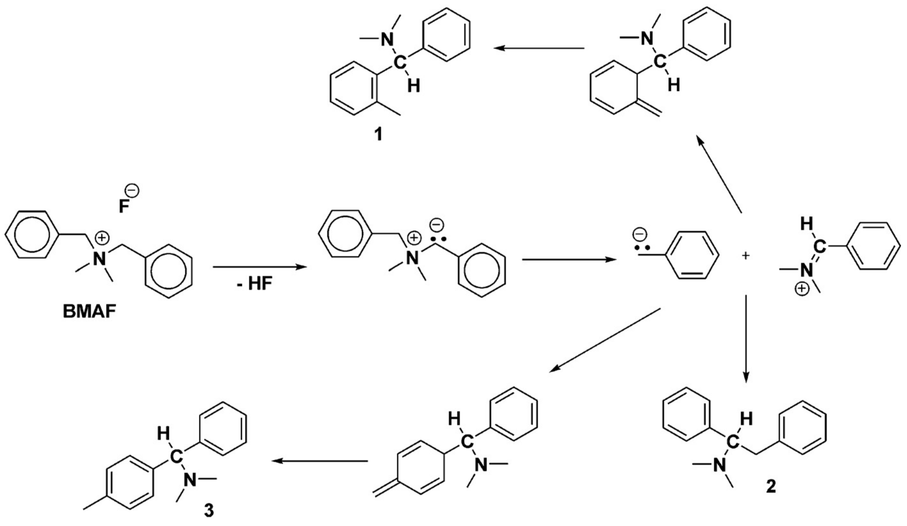

Scheme 3. Proposed mechanism of side reactions that may occur via intra-molecular rearrangements of BMAF ylide, formed by the abstraction of H atom by (F^-). This scheme is based on a published work where the ylide was generated by benzyllithium (Erling & Gary, 1967).

12 h, respectively. In THF, ca. 75 mol% (HF_2^-) was produced after 8 days. (Sharma & Fry, 1983) Although BMAF is not subject to Hofmann elimination (for lack of β-hydrogen atoms) all these R_4NF are subject, in principle, to elimination by the ylide mechanism, see 1D of Scheme 1.

We used ^{1}H-NMR to probe the occurrence/extent of side reactions. The spectrum of BMAF-0.1H_2O shows a few additional peaks, in comparison with that of BMABr-0.5H_2O (cf. Fig. SM-1). Although a detailed characterization of these side products is beyond the scope of the present work, their concentration can be calculated from peak areas. Assuming that the additional peaks were produced by intra-molecular rearrangements of BMAF ylide, see Scheme 3, some side products can be envisaged, namely, 1 (2.1, 2.2, 4.4, and 7.0–7.4 ppm), 2 (2.2, 2.9, 3.2, 4.1, and 6.9–7.4 ppm), and 3 (2.2, 2.3, 4.1, and 7.0–7.4 ppm); chemical shifts of (1–3) were calculated by available on-line software (Advanced Chemistry Development, 2013).

Compounds 1–3 have in common the presence of an *N*,*N*-dimethylamino group attached to a benzylic carbon atom. These methyl groups should have very close-, or identical chemical shifts. If the singlet at 2.08 ppm in the spectrum of BMAF-0.1H_2O is attributed to these methyl groups (part b of Fig. SM-1; relative area = 0.06) then the molar ratio BMAF/elimination products is 0.94/0.06, i.e., the extent of side reactions is, by this criterion, ca. 6 mol%.

3.3. Evaluation of the thermal stability of R_4NF-hydrates

For TBAF–3H_2O, mass decreases of 17.1 and 55.4% are expected due to the loss of water of hydration, and other volatiles (tributylamine and 1-butene), as shown in reactions 1 and 2 of Scheme 1 C. When TBAF·3H_2O is heated under reduced pressure at 77 °C for 15 h, the mass loss observed is 53% (Sharma & Fry, 1983), showing that the anhydrous electrolyte undergoes Hofmann elimination on heating, in agreement with previous discussion.

The following can be concluded from the TG/derivative thermogravimetry (DTG) of BMAF-0.1H_2O, Fig. 1a: (i) A mass loss of 1.5% occurs when the T reached 143 °C due, in part, to loss of water of hydration. (ii) Subsequently, the mass loss occurs in steps, from 143 to 175 °C (58.4%) and from 175 to 230 °C (40.0%); these ranges correspond to the DTG curve maxima at 171 and 217 °C, respectively. We seek an explanation for the appearance of the two peaks from the TG results of two tetraalkylammonium hydroxides. Such comparison is valid because F^- and OH^- anions are isoelectronics (Kluge & Weston, 2005). Whereas the curve of tetramethylammonium hydroxide pentahydrate (no β-hydrogens) shows peaks from 110 to 125 °C, and 125 to 130 °C, attributed to the ylide and S_N2-type decomposition mechanisms (Macomber, Boncella, Pivovar, & Rau, 2008), that of ethyltrimethylammonium deuteroxide hydrate

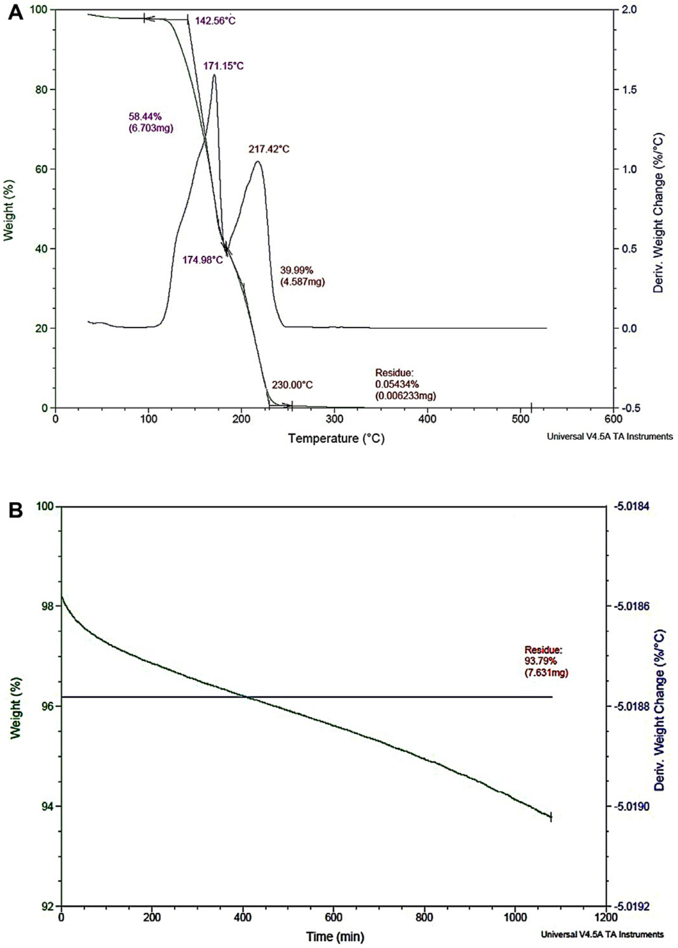

Fig. 1. (A) TG/DTG and (B) isothermal TG curves obtained for BMAF.0.1H_2O.

(β-hydrogens present), shows mass loss from 30 to 68 °C, due essentially to Hofmann elimination. Provided that the former quaternary ammonium hydroxide is a model for BMAF-0.1H_2O, we attribute the two consecutive peaks to degradation by the same mechanisms suggested.

Finally, the dependence of mass loss on time for BMAF-0.1H_2O is shown in Fig. 1b. A mass loss of 6% occurred after 18 h at 80 °C. The relevance of this result is that little electrolyte degradation occurs, even after its exposure to extreme conditions (high T and long time). Considering that R_4NF-hydrates are more stable in solution than in the solid state (the condition for the isothermal TG experiment) this thermal stability contrasts very favorably with the case of almost anhydrous TBAF, vide supra (Sharma & Fry, 1983).

3.4. Dissolution and acylation of cellulose in BMAF-0.1H_2O/DMSO

MCC and cotton cellulose form clear solutions in BMAF-0.1H_2O/DMSO. Table 1 shows the results of acylation of both celluloses, along with literature data for other R_4NF-hydrates/DMSO. The DS values obtained for the acylation in the former system (Entries 1 to 6) are higher than those reported for other electrolytes (Entries 7 and 8), although the DP of the cotton employed is more than double that acylated in TBAF–3H_2O (Ass et al., 2004; Casarano et al., 2011).

3.4.1. A rationale for the observed efficiency of BMAF-0.1H_2O

Considering the results of Table 1, the following question arises: What are the possible reasons for this efficiency? Note that for comparison, we employed conditions similar to those used for (TBAF–3H_2O) and (TAAF–H_2O), i.e., they may have not been optimized. Consequently, the differences in DS may have been larger.

In order to answer this question, and to understand the cellulose/R_4NF-hydrate/DMSO system we have carried out MD simulations of the interactions between the components presents. To our knowledge, this is the first time that MD simulations have been employed to probe the interactions in cellulose/R_4NF-hydate/DMSO solutions. Two systems were simulated, each containing 1100 DMSO molecules; one oligomer molecule, and either 24 molecules of BMAF plus 3 molecules of water (BMAF-0.1H_2O) or 24 molecules of TBAF plus 72 of water (TBAF–3H_2O). Details of these calculations are given in the Calculations section of *SM*. Table 2 summarizes the main results of these calculations.

Regarding the results of Table 2, the following is relevant:

(i) Calculation of the radial distribution function, RDF, of all atoms present around the oligomer surface has indicated that the extension of its solvation layer can be taken as equal to 0.5 nm; this value has been employed throughout;

(ii) Interactions of the oligomer with (F^-) and water are considered together. The extension of the oligomer solvation layer by (F^-), 0.122 to 0.196 nm, is not too far from the distances between (F^-) and water in crystals of hydrated inorganic electrolytes, calculated from X-ray diffraction (0.162–0.185 nm) (Simonov & Bukvetsky, 1978). On the other hand, the ratios (F^-/AGU) are 0.47, and 0.71, for BMAF-0.1H_2O and TBAF–3H_2O respectively (E2). Likewise, the number of hydrogen-bonds of the oligomer OH groups and (F^-) are 7, and 16, respectively (E3).

These differences do not necessarily mean that the (F^-/AGU) interactions are stronger for TBAF–3H_2O. The reason is that hydration of this anion leads to dramatic decrease in its basicity/nucleophilicty (Landini, Maia, & Rampoldi, 1989; Pliego & Pilo-Veloso, 2008), hence attenuates its interactions with the hydroxyl groups of the AGU. Thus (E6 and E7) of Table 2 show that the surface of the oligomer remains essentially anhydrous in the presence of BMAF-0.1H_2O. On the other hand, the oligomer is solvated by ca. 20 water molecules in case of TBAF–3H_2O. The RDF of the center of mass, COM, of these water molecules around the oligomer surface (Fig. SM-2) shows the presence of two peaks, with maxima at 0.182 nm and 0.298 nm, respectively. The number of water molecules associated with these peaks can be calculated from their areas. This calculation has indicated that the first peak is due to ca. 1.2 molecules, presumably due to water molecules that are hydrogen-bonded to the hydroxyl groups of the AGU. The second (broader) peak contains 18.7 water molecules. These are most certainly hydrogen-bonded to (F^-) of TBAF–3H_2O that is located within the solvation layer of the oligomer surface, giving anion hydration number of ca. 2 (an average hydration number of 4.7 for (F^-) has been deduced from MD simulations) (Öhrn & Karlström, 2004). As shown from NMR data of the system TBAF–water/MCC/DMSO, hydrogen bonding involves the hydroxyl groups of the AGU, (F^-) and water (Östlund, Lundberg, Nordstierna, Holmberg, & Nydén, 2009).

(iii) Our calculations have shown the following details of the interactions of these components. Fig. 2A shows a snapshot of the oligomer with DMSO (TBAF and water molecules not shown); part 2B shows the same snapshot in the presence of TBAF and DMSO (water molecules not shown); whereas 2C shows all system components. The arrows in parts 2B and 2C show that (F^-)

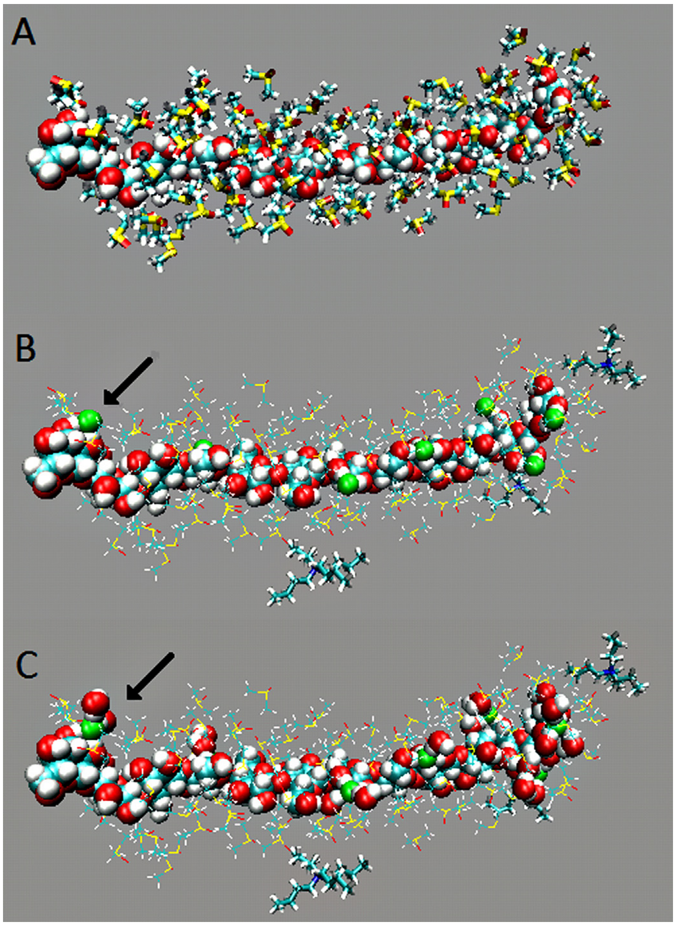

Fig. 2. Snapshots from the simulation of the system oligomer/TBAF–3H_2O/DMSO. The color codes employed are: green (F^-), red (oxygen), turquoise (carbon), blue (nitrogen), yellow (sulfur), and white (hydrogen). All three snapshots were taken from the same (simulation) frame. Part (A) shows the oligomer and the DMSO present in its solvation layer (0.5 nm). Part (B) shows DMSO and TBAF molecules. Part (C) shows all system components. The arrows in parts (B and C) show the simultaneous binding of (F^-) to two hydroxyl groups (AGU of the oligomer), and water molecules. (For interpretation of the references to color in this figure legend, the reader is referred to the web version of the article.)

Table 1
Results of acylation of MCC, and cotton cellulose, in BMAF.0.1H_2O/DMSO.[a]

Entry	Solvent[b]	Cellulose type	Carboxylic anhydride	Ester DS
1	BMAF-0.1H_2O/DMSO	MCC	Ethanoic	2.6
2	BMAF-0.1H_2O/DMSO	MCC	Butanoic	2.1
3	BMAF-0.1H_2O/DMSO	MCC	Hexanoic	2.5
4	BMAF-0.1H_2O/DMSO	Cotton	Ethanoic	2.4
5	BMAF-0.1H_2O/DMSO	Cotton	Butanoic	2.0
6	BMAF-0.1H_2O/DMSO	Cotton	Hexanoic	2.5
7[c]	TAAF–H_2O/DMSO	MCC	Ethanoic	1.9
8[d]	TBAF–3H_2O/DMSO	Cotton	Ethanoic	1.6–2.3

[a] Experimental conditions: 3 h; 80 °C; carboxylic anhydride/AGU molar ratio = 6; MCC, DP_V = 175; cotton cellulose, DP_v = 920.

[b] The amounts employed were: cellulose, 0.5 g (3.08 mmol); DMSO, 40 mL (0.56 mol); BMAF-0.1H_2O, 3.3 g (13.35 mmol); BMAF/AGU molar ratio = 4.3.

[c] Literature data. Conditions: TAAF = 15.33 mmol; DMSO = 0.42–0.56 mol; TAAF/AGU molar ratio = 5.0; based on 0.5 g cellulose, 30–40 mL DMSO, and 3.3 g TAAF–H_2O; 3 h, 80 °C; ethanoic anhydride/AGU molar ratio = 6; MCC, DP_V = 175 (Casarano et al., 2011).

[d] Literature data. Conditions: TBAF = 20.92 mmol; DMSO = 0.84 mol; TBAF/AGU molar ratio = 3.4; based on 1 g cellulose, 60 mL DMSO, and 6.6 g TBAF–3H_2O; 3 h, 60–100 °C; ethanoic anhydride/AGU molar ratio of 6; cotton cellulose, DP_v = 440 (Ass et al., 2004).

Table 2
Results of MD simulations.[a]

Entry	Results obtained	BMAF-0.1H_2O	TBAF–3H_2O
Fluoride ion-oligomer interactions			
E1	Extension of the oligomer first solvation shell by (F^-)	From 0.122 to 0.190 nm; maximum at 0.146 nm	From 0.128 to 0.196 nm; maximum at 0.148 nm
E2	Number and distribution of (F^-) at the oligomer surface	5.64 F^- (0.47 F^-/AGU) 0.84 F^-/AGU-C2-OH 0.72 F^-/AGU-C3-OH 0.24 F^-/AGU-C6-OH	8.52 F^- (0.71 F^-/AGU) 1.2 F^-/AGU-C2-OH 1.2 F^-/AGU-C3-OH 0.6 F^-/AGU-C6-OH
E3	Number of hydrogen-bonds per (simulation) frame between the oligomer OH groups and F^-	7 ± 3	16 ± 2
Electrolyte cation-oligomer interactions			
E4	Extension of the oligomer solvation shell by electrolyte-cation	From 0.268 to 0.594 nm, with maximum at 0.404 nm	From 0.294 to 0.564 nm, with maximum at 0.386 nm
E5	Number of cations at oligomer surface	4.68 BMA^+ (0.39 BMA^+/AGU)	2.04 TBA^+ (0.17 TBA^+/AGU)
Water-oligomer interactions			
E6	*Number* of H_2O molecules at oligomer surface	None	20.04 H_2O (1.67 H_2O/AGU)
E7	*Number* of hydrogen-bonds per frame between the oligomer OH groups and water	None	1 ± 1
DMSO-oligomer interactions			
E8	Number of DMSO molecules at oligomer surface	91.2 DMSO (7.6 DMSO/AGU)	84 DMSO (7.0 DMSO/AGU)
System component interactions, *excluding the oligomer*			
E9	Number of H-bonds between H_2O and (F^-) inside the oligomer solvation shell (0.5 nm)[b]	None	15 ± 2
E10	Number of DMSO per (F^-)	7.3	12.1
E11	Distance between F^- and the N^+ of the electrolyte cation	From 0.284 to 0.486 nm, with maximum at 0.338 nm	From 0.314 to 0.534 nm, with maximum at 0.374 nm
E12	Distance between S of DMSO and (F^-)	From 0.262 to 0.560 nm, with maximum at 0.462 nm	From 0.272 to 0.618 nm, with maximum at 0.468 nm

[a] (Species) numbers and distances listed are average values, calculated for the simulation time interval 15–70 ns.

[b] This number is given per (simulation) frame, corresponding to 0.005 ns simulation time.

is simultaneously associated with the hydroxyl groups of the AGU and water. That is, this anion is acting as a "bridge", leading to (HOH ··· F^- ··· HO-AGU).

(iv) The results of E4 and E5 may be explained on the bases of differences in the hydration of (F^-) and volumes of the cations (0.389 and 0.286 nm^3, for TBA^+ and BMA^+, respectively). Thus anion hydration leads to weaker anion-cation interactions in TBAF–3H_2O relative to that of BMAF-0.1H_2O. Consequently, the oligomer solvation layer of the former electrolyte is thinner and contains a smaller number of cations, because it contains water instead of the voluminous TBA^+, E6;

(v) Explanation of E8 to E12 rests on two known facts: (a) the free energy of transfer of (F^-) from water (or protic solvents in general) to DMSO is positive, i.e., unfavorable (Hefter, 1991, 1997), (b) water–DMSO interactions are stronger than water–water counterparts (Kingston & Symons, 1973; Mizuno, Imafuji, Ochi, Ohta, & Maeda, 2000; Shashkov, Kiselev, Tioutiounnikov, Kiselev, & Lesieur, 1999; Symons, 1986). Accordingly, water is expected to interact strongly not only with the fluoride ion, but also with DMSO (E 10), at the expense of interactions of the latter with the other components of the system. This is clearly shown by E8 (more DMSO molecules are present at the surface of the oligomer-BMAF-0.1H_2O), and E12 (the distance (DMSO-F^-) is larger for TBAF–3H_2O. The results reported in E11 can be explained based on the volume of the two cations, vide supra. For example, quantum mechanics calculations (Pliego & Pilo-Veloso, 2008) have shown that the distance (F^- ··· N^+) increases as a function of increasing the cation volume.

In summary, the efficiency of R_4NF/DMSO as solvents for cellulose is due to, in part, the simultaneous hydrogen bonding of (F^-) to C2—OH and C3—OH, as shown by the arrow in parts (B and C) of Fig. 2. Based on our calculations, the water in TBAF–3H_2O probably affects the electrolyte performance as a solvent for cellulose, due to the solvation of (F^-). This presumably affects the physical state of dissolved cellulose, because of the resulting weaker interactions of (F^-) with the hydroxyl groups of AGU. In this regard, BMAF-0.1H_2O offers an advantage because of its much lower water content, and smaller volume. It is also important to take into account the thermal stability of these R_4NF-hydrates, and the deleterious effects of water on the reaction outcome (hydrolysis of acyl chlorides and anhydride, hydrolysis of produced ester). A corollary to the more extensive interaction of BMAF with cellulose is that the biopolymer in this system is probably more accessible, hence more reactive; this agrees with the higher DS obtained. We plan to study further this point, i.e., the dependence of product DS on biopolymer accessibility, hence reactivity.

4. Conclusions

A new quaternary ammonium fluoride-hydrate, BMAF-0.1H_2O, was synthesized by a simple procedure. The thermal stability of this electrolyte is satisfactory; it dissolves MCC and fibrous cellulose easily; the DS of the esters obtained are comparable, or higher than those obtained with TAAF–H_2O and TBAF–3H_2O under comparable experimental conditions. The reasons for the relative efficiency of BMAF-0.1H_2O have been deduced from the results of MD simulations, available for the first time for these solvent systems. These have shown that the (F^-) of TBAF–3H_2O is solvated by the water present leading, presumably, to a decrease in its basicity and hydrogen-bonding ability with the hydroxyl groups of the AGU (lower biopolymer accessibility, hence reactivity). The introduction of BMAF-0.1H_2O is welcomed not only for cellulose dissolution/derivatization, but also for organic synthesis in general.

Acknowledgments

We thank the FAPESP (State of São Paulo Research Foundation) for financial support and a postdoctoral fellowship to R. Casarano; the CNPq (National Council for Scientific and Technological Research) for a productivity fellowship to O. A. El Seoud; Mariana C. Lucats and Cezar Guizzo for their help. This work has been carried out within the frame of INCT-Catálise.

Appendix A. Supplementary data

Supplementary data associated with this article can be found, in the online version, at http://dx.doi.org/10.1016/j.carbpol.2013.09.043.

References

Advanced Chemistry Development, I. A. L. (2013). *NMR Predictors V. 11.01. Scifinder Scholar*. http://scifinder.cas.org [accessed 17.11.12]

Albanese, D., Landini, D., & Penso, M. (1998). Hydrated tetrabutylammonium fluoride as a powerful nucleophilic fluorinitaing agent. *Journal of Organic Chemistry*, *63*, 9558–9589.

Armagero, W. L. F, & Chai, C. L. L. (2003). *Purification of laboratory chemicals* (5th ed.). New York: Elsevier.

Ass, B. A. P., Frollini, E., & Heinze, T. (2004). Studies on the homogeneous acetylation of cellulose in the novel solvent dimethyl sulfoxide/tetrabutylammonium fluoride trihydrate. *Macromolecular Bioscience*, *4*, 1008–1013.

ASTM Standard D1795-96. (2007). *Standard test methods for intrinsic viscosity of cellulose*. West Conshohocken, PA: ASTM International. http://dx.doi.org/10.1520/D1795-96

ASTM Standard D871-96. (2004). *Standard test methods of testing cellulose acetate*. West Conshohocken, PA: ASTM International. http://dx.doi.org/10.1520/D0871-96

Busi, S., Lahtinen, M., Ropponen, J., Valkonen, J., & Rissanen, K. (2004). Synthesis, characterization and thermal properties of new aromatic quaternary ammonium bromides: Precursors for ionic liquids and complexation studies. *Journal of Solid State Chemistry*, *177*, 3757–3767.

Casarano, R., & El Seoud, O.A. (2013). Solvent system, a process for producing a solvent system and its use. Patent 001097-9[pending]. BR 10.

Casarano, R., Nawaz, H., Possidonio, S., da Silva, V. C., & El Seoud, O. A. (2011). A convenient solvent system for cellulose dissolution and derivatization: Mechanistic aspects of the acylation of the biopolymer in tetraallylammonium fluoride/dimethyl. *Carbohydrate Polymers*, *83*, 1285–1292.

Chempath, S., Boncella, J. M., Pratt, L. R., Henson, N., & Pivovar, B. S. (2010). Density functional theory study of degradation of tetraalkylammonium hydroxides. *Journal of Physical Chemistry C*, *114*, 11977–11983.

Cox, D. P., Terpinski, J., & Lawrynowicz, W. (1984). Anhydrous tetrabutylammonium fluoride: A mild but highly efficient source of nucleophilic fluoride ion. *Journal of Organic Chemistry*, *49*, 3216–3219.

Erling, G., Jr., & Gary, W. (1967). Carbanions. IX. Evidence for a duality of mechanism in rearrangement of carbanions. *Journal of the American Chemical Society*, *89*, 1852–1862.

Fieser, L. F. (1967). *Fieser and Fieser's reagents for organic synthesis*. New York: Wiley.

Hefter, G. T. (1991). Fluoride solvation. The case of the missing ion. *Pure and Applied Chemistry*, *63*, 1749–1758.

Hefter, G. T. (1997). Solvation of fluoride ions 4. Gibbs energies of transfer from water to aqueous dimethylsulphoxide, propanone and 2-methylpropan-2-ol mixtures. *Journal of Molecular Liquids*, *73-74*, 267–276.

Heinze, T., & Koehler, S. (2010). *Dimethyl sulfoxide and ammonium fluorides – Novel cellulose solvents*. *ACS Symposium Series* (Vol. 1033) (Cellulose Solvents).

Heinze, T., Lincke, T., Fenn, D., & Koschella, A. (2008). Eficient allylation of cellulose in dimethyl sulfoxide/tetrabutylammonium fluoride trihydrate. *Polymer Bulletin (Berlin)*, *61*, 1–9.

Heinze, T., Wanga, Y., Koschella, A., Sullob, A., & Foster, T. J. (2012). Mixed 3-mono-O-alkylcellulose: Synthesis, structure characterization and thermal properties. *Carbohydrate Polymers*, *90*, 380–386.

Karoly, N., & Gyermek, G. (1952). Synthesis of compounds with ganglion-blocking effects. I. Synthesis of some simple quaternary ammonium derivatives. *Acta Chimica Academiae Scientiarum Hungaricae*, *2*, 95–101.

Kingston, B., & Symons, M. C. R. (1973). Solvation spectra. Part 44.-Nuclear magnetic resonance study of binary solvent mixtures: Water structural effects. *Journal of the Chemical Society, Faraday Transactions 2: Molecular and Chemical Physics*, *2*(69), 978–992.

Kluge, S., & Weston, J. (2005). Can a hydroxide ligand trigger a change in the coordination number of magnesium ions in biological systems? *Biochemistry*, *44*, 4877–4885.

Koehler, S., & Heinze, T. (2007). New solvents for cellulose: Dimethyl sulfoxide/ammonium fluorides. *Macromolecular Bioscience*, *7*, 307–314.

Landini, D., Maia, A., & Rampoldi, A. (1989). Dramatic effect of the specific solvation on the reactivity of quaternary ammonium fluorides and poly(hydrogen fluorides), (HF), in media of low polarity. *Journal of Organic Chemistry*, *54*, 328–332.

Leibert, T. F., & Heinze, T. (2005). Tailored cellulose esters: Synthesis and structure determination. *Biomacromolecules*, *6*, 333–340.

Macomber, C. S., Boncella, J. M., Pivovar, B. S., & Rau, J. A. (2008). Decomposition pathways of an alkaline fuel cell membrane material component via evolved gas analysis. *Journal of Thermal Analysis and Calorimetry*, *93*, 225–229.

Makosza, M., & Chesnokov, A. A. (2003). Study of the mechanism of base induced dehydrobromination of *trans*-β-bromostyrene. *Tetrahedron*, *59*, 1995–2000.

Mizuno, K., Imafuji, S., Ochi, T., Ohta, T., & Maeda, S. (2000). Hydration of the CH groups in dimethyl sulfoxide probed by NMR and IR. *Journal of Physical Chemistry B*, *104*, 11001–11005.

Öhrn, A., & Karlström, G. (2004). A combined quantum chemical statistical mechanical simulation of the hydration of Li^+, Na^+, F^-, and Cl^-. *Journal of Physical Chemistry B*, *108*, 8452.

Östlund, Å., Lundberg, D., Nordstierna, L., Holmberg, K., & Nydén, M. (2009). Dissolution and gelation of cellulose in TBAF/DMSO solutions: The roles of fluoride ions and water. *Biomacromolecules*, *10*, 2401–2407.

Pliego, J. R., & Pilo-Veloso, D. (2008). Effects of ion-pairing and hydration on the SNAr reaction of the F- with p-chlorobenzonitrile in aprotic solvents. *Physical Chemistry Chemical Physics*, *10*, 1118–1124.

Sharma, R. K., & Fry, J. L. (1983). Instability of anhydrous tetra-n-alkylammonium fluorides. *Journal of Organic Chemistry*, *48*, 2112–2114.

Shashkov, S. N., Kiselev, M. A., Tioutiounnikov, S. N., Kiselev, A. M., & Lesieur, P. (1999). The study of DMSO/water and DPPC/DMSO/water system by means of the X-ray, neutron small-angle scattering, calorimetry and IR spectroscopy. *Physica B: Condensed Matter (Amsterdam)*, *271*, 184–191.

Simonov, V. I., & Bukvetsky, B. V. (1978). On the geometry of O—H ··· F hydrogen bonds in metal fluoride hydrates. *Acta Crystallographica, Section B: Structural Science*, *34*, 355–358.

Sun, H. R., & DiMagno, S. G. (2005). Anhydrous tetrabutylammonium fluoride. *Journal of the American Chemical Society*, *127*, 2050–2051.

Sun, H. R., & DiMagno, S. G. (2006). Room-temperature nucleophilic aromatic fluorination: Experimental and theoretical studies. *Angewandte Chemie, International Edition in English*, *45*, 2720–2725.

Symons, M. C. R. (1986). Infrared and NMR studies of probes in binary solvent systems. *Pure and Applied Chemistry*, *58*, 1121–1132.

Tutaj, B., Gonzalez-Perez, A., Czapkiewicz, J., Del Castillo, J. L., & Rodriguez, J. R. (2001). Apparent molar volumes of benzyltrimethylammonium bromide and its homologs in aqueous solution at 15, 25, and 35 °C. *Journal of Solution Chemistry*, *30*, 1101–1109.

Xu, D., & Edgar, K. J. (2012). TBAF and cellulose esters: Unexpected deacylation with unexpected regioselectivity. *Biomacromolecules*, *13*, 299–303.

Xu, D., Li, B., Tate, C., & Edgar, K. J. (2011). Studies on regioselective acylation of cellulose with bulky acid chlorides. *Cellulose*, *18*, 405–419.

Zheng, X., Gandour, R. D., & Edgar, K. J. (2013). Probing the mechanism of TBAF-catalyzed deacylation of cellulose esters. *Biomacromolecules*, *14*, 1388–1394.